Theses and Dissertations

Graduate School

2019

Illumination of the Golgi apparatus of Pathogenic and Nonpathogenic Naegleria species

Tyler M. Poe
Virginia Commonwealth University

Illumination of the Golgi apparatus of Pathogenic and Nonpathogenic *Naegleria* species

A thesis submitted in partial fulfillment of the requirements for the degree of Master of Science
at Virginia Commonwealth University

By

Tyler Matthias Poe
Bachelor of Science, Virginia Commonwealth University, 2019

Principle Investigator: Dr. Francine Marciano-Cabral
Professor, Department of Microbiology and Immunology

Virginia Commonwealth University
Richmond, Virginia,
August, 2019

<u>Acknowledgements</u>

Table of Contents   **Page Number(s)**

ILLUMINATION OF THE GOLGI APPARATUS OF PATHOGENIC AND NONPATHOGENIC *NAEGLERIA* SPECIES

BY Tyler Poe, Bachelor of Science

A thesis submitted in partial fulfillment of the requirements for the degree of Master of Science at Virginia Commonwealth University

Virginia Commonwealth University, 2019

Principle Investigator: Dr. Francine Marciano-Cabral, Professor, Department of Microbiology and Immunology

Abstract

In this study, *Naegleria fowleri*, a pathogenic amoeba and the causative agent of Primary Amebic Meningoencephalitis (PAM), was utilized to determine the presence or absence of classically conserved Golgi molecules featured in the expression of a Golgi apparatus. Previous studies concluded no Golgi expression via light microscopy and transmission electron microscopy, but a recent report on *Naegleria gruberi* indicated the presence of dispersed Golgi tubules. Non-pathogenic species of the *Naegleria* genus such as *Naegleria gruberi* 30540 and *Naegleria lovaniensis* 30569 were utilized in Western immunoblot analysis compared to reduced whole-cell lysate proteins of two strains of *N. fowleri* and Vero CCL-81, *Chlorocebus* sp. kidney epithelial cells, which were utilized as a positive control for Golgi expression. *N. fowleri* and *N. lovaniensis* whole-cell lysates had indications of a 110 kDa reduced protein, associated with the predicted molecular weights of the beta-COPI subunit of the COPI cis-Golgi vesicular transport complex with further Western immunoblot indication of a weak band around 25 kDa corresponding to rabbit polyclonal antibodies specific for ARF1. Serial Dilutions of Wheat Germ Agglutinin Alexa Fluor 488[TM] were performed on Vero cells, *Naegleria fowleri* 30894, and *N. gruberi 30540* with 1:100 dilution of recommended stock dilution of WGA 488 determined for utilization in sequential immunofluorescence. Sequential immunofluorescence with Wheat Germ

Agglutinin Alexa Fluor 488[TM] and then blocked with 3% BSA:PBS [wt/vol] dilution with subsequent incubation in rabbit anti-beta-COPI primary 1:250, and 1:1000 of Alexa Fluor 594 goat anti-rabbit secondary antibody exposure showed strong indications of organized cis- and trans-punctate Golgi body markers in close association in individual and dividing cells of *Naegleria fowleri* and conserved Golgi expression in the positive control Vero cells, but further experiments are necessary to verify this finding with *N. fowleri*.

<u>Introduction</u>

In 1898, the Golgi apparatus was discovered by Camillo Golgi and viewed as a stack of flattened membranes via visual examination by light microscopy. The Golgi apparatus is a eukaryotic, cellular organelle responsible for the N- and O-glycosylation of proteins and subsequently accountable for membrane trafficking toward the plasma membrane, known as anterograde transport, and away from the plasma membrane, known as retrograde transport (Lodish *et al*., 2000; Popoff *et al*., 2011). Within the confines of this organelle, specific Golgi protein complexes and regulators are highly conserved in eukaryotic cells as well as mammalian cells and possibly *Naegleria* species, based on *in silico* DNA prediction of *Naegleria fowleri* CDC:V212 genomic data, proteins such as ADP ribosylation factors (ARF) and coatomer protein complex 1 (COPI) (Herman *et al*., 2018; Nickel *et al*., 2002; Nikel *et al.*,1982). However, there have been no transmission electron microscopy or light microscopy studies that have differentiated individual vacuoles or any indication of a defined Golgi apparatus in *Naegleria fowleri* due to concentric focus on treating the organism, rather than understanding its polymorphic cell biology (Martínez-Castillo *et al*., 2016; González-Robles *et al*., 2009).

Regardless of morphology, these protein complexes of the Golgi form to produce budding vesicles for participation in membrane and intracellular trafficking. Specifically, COPI is a protein coatomer complex, analogous to clathrin, and is comprised of seven subunits involved in initiating retrograde transport of vesicles within the cisternae of the Golgi apparatus in mammalian cells and insect cells (Nickel *et al.,* 2002*;* Jayaram *et al.,* 2008; Popoff *et al.,* 2011). Within this coatomer complex is the beta subunit of COPI with a molecular weight of ~110 kiloDaltons (kDa) and this complex was verified by previous research to have *in silico* predicted subunits for *N. fowleri* (Herman *et al*., 2018). Whereas Adenosine diphosphate-ribosylation factors (ARF) are members of the ARF family of Guanosine Triphosphate-binding (GTP) proteins that belong to the Ras superfamily of small GTPases, regulating a broad range of

biological processes (Muthamilarasan *et al.,* 2016). ARF1 initiates the COPI complex via hydrolysis of GTP, also found *in silico* predicted orthologues for *Naegleria* sp. (Muthamilarasan *et al.,* 2016; Herman *et al*., 2018). ARFs are found ubiquitously in all eukaryotic cells and are greatly conserved, sharing a greater than 60% sequence homology and a molecular weight of 18 to 25 kDa, with post-translational modifications possible (Muthamilarasan *et al.,* 2016; Herman *et al*., 2018).

Regardless of conserved proteins, many forms of Golgi complexes have been described in various yeast strains. Dispersed cisternae in *Saccharomyces cervisiae* and multiple compartmental Golgi apparatuses are found within *Pichia pistoris* (Suda and Nakano, 2012). More recently, a study published in 2018 indicated the morphology of *Naegleria gruberi*'s Golgi apparatus was characterized by dispersed, tubular compartments according to Herman *et al.*, 2018 when utilizing antibodies specific toward the *N. gruberi* cis-Golgi and Endoplasmic Reticulum markers.

Naegleria fowleri is a pathogenic, free-living amoeba that can be found in freshwater ponds, lakes, and hot springs (Eddy *et al.,* 2009; Cope and Ali*,* 2016). Although infection is rare, the amebic inoculation is often fatal in greater than 97% of acquired cases (Zysset-Burri *et al*., 2014). *N. fowleri* is the causative agent of Primary Amebic Meningoencephalitis (PAM) after passage through the nasal canal with water containing the potentially fatal trophozoite (Cope and Ali, 2016; Martinez, 1985). *N. fowleri* has recently been associated with two fatal cases of PAM in Minnesota in 2010 and 2012, which represents a novel geographical concentration and emergence than the majority of cases found in the southern states of the United States (Cope and Ali, 2016). Ablution of nasal rinses has also been associated with three cases of PAM (Hunte *et al.,* 2013). These occurrences facilitate a necessity to understand the cell biology of the organism for potential intracellular drug targeting of *Naegleria* sp. if the Golgi is distinct enough from the mammalian Golgi apparatus or for future studies utilizing brefeldin A for vesicular targeting (Cope and Ali*,* 2016; Fritz-Laylin, 2010; Herman *et al*., 2018).

While *N. fowleri* is the primary focus in the medical field, *Naegleria lovaniensis* and *N. gruberi* represent free-living, nonpathogenic species of amoeba within the genus, which are also closely associated with freshwater bodies and both are ubiquitous in distribution (Jamerson *et al.,* 2012; Zysset-Burri *et al*., 2014). *N. lovaniensis* is more closely related to *N. fowleri* than *N. gruberi* in genomic studies (Zysset-Burri *et al*., 2014). While distinct members of the genus, non-pathogenic amoebas have limited microscopic and morphological studies in electronic-based journals. In this study, Vero cells, African green monkey kidney epithelial cells of the *Chlorocebus* species, were utilized as a mammalian comparison for the structure of the Golgi apparatus, particularly used in various viral models, and was available for utilization as a positive control (Mackenzie *et al.,*1999; Rohde *et al.,* 2012, Osada *et al.,* 2014).

Wheat germ agglutinin (WGA) Alexa Fluor[TM] 488 was utilized for the amebic study, a nonspecific lectin probe for Golgi localization that binds to N-acetylglucosamine and sialic acids with specificity toward the trans-Golgi in fixed cells and registers green when visualized through confocal microscopy via laser excitation at ~495-519 nm (Chazotte, 2011), along with beta-COPI rabbit polyclonal IgG antibody, a potential probe for cis-Golgi localization, with effort in use of dual probes for sequential staining to elucidate the Golgi apparatus structure. This research proposes a conservative approach to Golgi apparatus elucidation based on polyclonal antibodies and lectins as a method of detection for orthologous membrane transport vesicles present in the Golgi apparatus via confocal laser microscopy after Western immunoblotting confirmation.

Materials and Methods

Cell Culture

For use in protein investigation and use in microscopy, amoeba purchased from the American Type Culture Collection such as *N. fowleri* (ATCC 30894), *N. gruberi* (ATCC 30540), *N. lovaniensis* (ATCC 30569), and a CDC strain of *N. fowleri* known as V212 were all grown in Tissue culture flasks (75-cm^2) containing Oxoid medium, which consists of: 0.55% [wt/vol] Oxoid neutralized liver digest, 0.3% [wt/vol] dextrose, 0.5% [wt/vol] proteose peptone, 0.25% [wt/vol] yeast extract in 1X Page's saline. Additional 1% [vol/vol] Fetal Calf Serum (GIBCO, Grand Island, NY) and 0.1% Hemin in 1N NaOH [wt/vol] were added to the final volume (Cline *et al.* 1983). Cells were cultured at 37°C for *N. fowleri* strains and 33°C for *N. lovaniensis* and *N. gruberi*, representing a novel growth temperature for *N. gruberi* in Oxoid media compared to previous methodology (Schuster, 2002; Herman *et al*., 2018; Jamerson *et al.,* 2012; Marciano-Cabral *et al*., 1982).

Vero (ATCC CCL-81) cells, African green monkey kidney epithelial cells, were cultured in Tissue culture flasks (75-cm^2) at 37°C in ~5% CO_2 atmosphere using Dulbecco's Modified Eagle Medium (DMEM) (GIBCO, Grand Island, NY), filter-sterilized with sterile Acrodisc® PF Syringe Filters consisting of 0.8/0.2 µm pores (Life Sciences, Fribourg, Switzerland), completed with the following additions: 0.87% [vol/vol] cellgro® 100X Non-essential Amino Acids (Mediatech, Manassas, VA), 0.87% [vol/vol] cellgro® 100 mM Sodium Pyruvate (Mediatech, Manassas, VA), 0.87% [vol/vol] Pen Strep (GIBCO, Grand, NY), 0.87% [vol/vol] 200 mM L-glutamine, 0.87% [vol/vol] 100X MEM Vitamin solution (GIBCO, Grand, NY), and 8.7% [vol/vol] Fetal Bovine Serum (GIBCO, Grand Island, NY), with the addition of 10 mM [wt/vol] HEPES to the final volume.

Whole Cell Lysates

For use in 4X Laemmli Reducing Lysis Buffer to examine respective amebic whole cell lysate proteins for Western Blot analysis, lysates of *N. lovaniensis* (ATCC 30569), *N. fowleri* (ATCC 30894 - Lee), *N. fowleri* CDC: V212, *N. gruberi* (ATCC 30540), Vero (ATCC CCL-81), were utilized in this study. Tissue culture flasks 75-cm^2 of confluent cells were perturbed by mechanical force to remove adhered cells and their respective supernatant deposited into sterile 50 mL conical tubes for centrifugation. Vero cells were removed with a sterile spatula before depositing into a sterile 50 mL conical tube, with additional completed DMEM added before centrifugation.

Conical tubes 50 mL containing cells were utilized for initial centrifugation at 1250 rpm for 5 minutes at 23°C with an Eppendorf Centrifuge 5810 R and the supernatant removed and subsequent pellets re-suspended in sterile 1.5 mL microcentrifuge tubes containing 1 mL of 1X Phosphate Buffered Saline at pH 7.4 (Quality Biological, Gaithersburg, MD). After three centrifugal cycles and the third subsequent re-suspension in 1X PBS, Roche™ mammalian protease inhibitor cocktail (SIGMA, St. Louis, MO) was added after thawing and vortexing at a 1:100 ratio to respective lysate samples. Additional DNase 1 (Worthington, Lakewood, NJ) (10 mg/mL) and 100 mM phenylmethylsulfonyl fluoride (PMSF) in dimethyl sulfoxide (DMSO) at 1:1000 were added to Vero cells.

Finally, all lysates endured three freeze-thaw cycles in liquid nitrogen and subsequent 5-minute duration thaw in a 37°C water bath. Vero cells were homogenized using a 26.5 gauge sterile needle aspiration 30 times. Samples were vortexed after thawing and aliquoted into sterile 0.5 mL microcentrifuge tubes and stored in -80°C for experimentation.

Western immunoblotting

Protein concentrations of whole-cell lysates were measured within 24 hours prior to Western procedure via Bradford Assay (Bradford, 1976; Kruger, 1996) and stored in -20°C for 18-20 hours. Absorbance was measured via 96-well plates (Corning Costar) using the SoftMax Pro 6.4 software on a SpectraMax M3 prior to each 4X Sodium Dodecyl Sulfate (SDS) Laemmli Reducing Lysis Buffer preparation for use in polyacrylamide gel electrophoresis.

After preparation of the respective lysate in a 3:4 ratio with deionized water (DiH_2O) in remaining 1:4 of 4X Laemmli Reducing Lysis Buffer and adjusted to respective microgram target of whole-cell lysate sample with the additional DiH_2O (Quality Biological, Gaithersburg, MD), each respective sample was loaded into a gel lane and electrophoresed at 200V for 12% Novex Wedgewell Tris-Glycine gels (Invitrogen, Carlsbad, CA) or 8% Novex Wedgewell Tris-Glycine gels (Invitrogen, Carlsbad, CA) for approximately 40 minutes until the dye front reached the bottom. Gels were then transferred onto a nitrocellulose membrane at 10V for 1 hour for precast gels. Immunoblots were placed on a rocker and were blocked in 5% [wt/vol] Non-fat Dry Milk Pro-blotting Grade Blocker (Bio-Rad) in a 0.1% Tris-buffered Saline-Tween (TBST) solution for one hour at room temperature.

Western blots were then subjected to a 1:1000 primary antibody of either polyclonal Rabbit anti-beta-COPI IgG (Novus Biologicals, Littleton, CO), polyclonal Rabbit anti-Arf1 IgG (Novus Biologicals, Littleton, CO) or polyclonal Rabbit anti-beta-actin IgG (Invitrogen, Rockford, IL) for overnight exposure (~16-18 hours). Six five-minute washes of 0.1% TBST were conducted to remove nonspecific background. Next, Goat anti-Rabbit IgG (H+L) Superclonal™ secondary antibody (Invitrogen, Bengaluru, India), Horseradish Peroxidase conjugate IgG, was applied in a 1:10,000 dilution for 1 hour at room temperature. Another six five-minute washes of 0.1% TBST was applied. Next, Pierce™ Enhanced Chemiluminescent (ECL) Western Blotting (Thermo Scientific, Rockford, IL) substrate reagents 1 and 2 were combined at 1:1 and applied to the Western immunoblot. Western immunoblots were subjected to 20-minute exposures on

BioExcell® X-ray film (World Wide Medical Products, Mortsel, Belgium) in a dark room to maximize signal for polyclonal antibody detection. Films were processed with the Kodak X-OMAT 2000A Processor maintained by Virginia Commonwealth University.

Western Blot Photo-capture Procedure

Images of western immunoblots captured with X-ray film (World Wide Medical Products, Mortsel, Belgium) were scanned using an HP 2656 scanning printer utilizing the HP Easy Scan application with films placed on a white paper background and then converted to grayscale in Adobe Photoshop and cropped and saved as .tif files.

WGA Serial Dilution Immunofluorescence

For use in Wheat Germ Agglutinin immunofluorescence assays, amoeba containing flasks were perturbed with mechanical force to remove adherent cells into the supernatant and poured into 50 mL conical tubes for centrifugation at 1250 rpm for 5 minutes. Vero cells underwent centrifugation cycles after the addition of 0.25% [vol/vol] Trypsin, in Ethylenediaminetetraacetic acid (EDTA), utilized to remove the cells and complete DMEM utilized directly after to inhibit Trypsin. After removal of the supernatant and subsequent re-suspension in 1X PBS (GIBCO, Grand Island, NY) lacking Calcium Chloride and Magnesium Chloride, another centrifugation at 1250 rpm for 5 minutes was performed and subsequent supernatant removed and cells incubated in 2% paraformaldehyde:PBS to be vortexed and dispersed onto slides for heat fixation at 37°C for 15 minutes. Slides were washed with Hank's Balanced Salt Solution (HBSS) three times. The Wheat Germ Agglutinin Alexa Fluor™ 488 conjugate lectin (Invitrogen, Eugene, OR) probe was prepared from solution of 1 mg/mL in 1X PBS to the recommended 5 µg/mL in 1X HBSS, designated as "Stock" in this study. Serial dilutions of the labeling solution were prepared in 1X HBSS. Slides were incubated with respective labeling dilution for 10 minutes at room temperature. Slides were then washed twice with 1X HBSS and mounted with 10 µL of Vectashield containing DAPI (Vectashield,

Burlingame, CA) (Wang *et al.*, 2010). Slides were analyzed and captured using a Zeiss 710 Confocal Laser Microscope maintained by Virginia Commonwealth University.

Sequential Immunofluorescence

In order to determine whether the Golgi apparatus could be identified with two probes for colocalization, the initial previously stated and modified protocol for WGA 488 serial dilutions were performed up until the mounting process (Wang *et al.,* 2010). After the two subsequent washes in 1X HBSS, cells were submerged and permeabilized with -20°C methanol for 5 minutes. After methanol permeabilization, slides were incubated with three 5 minute exposures to ice-cold 1X PBS and rinsed three times with 1X PBS before blocking with 3% Bovine Serum Albumin in PBS for 30 minutes. Primary Rabbit anti-beta-COPI polyclonal IgG 1:250 or 3% BSA:PBS 1:250 was distributed among slides and incubated for 1 hour at room temperature to respective trial and control slides. Slides were then incubated for three five-minute incubations of 1X PBS and then washed three times with 1X PBS. Next, a 1:1000 dilution of Alexa Fluor 594 Goat anti-Rabbit conjugate antibody (Invitrogen, Eugene, OR) was administered for 1 hour at room temperature. Slides were incubated with three 5-minute exposures to 1X PBS and rinsed three times each with 1X PBS and mounted with Vectashield containing DAPI (Vectashield, Burlingame, CA). Slides were analyzed at 1 Airy Unit, a measurement for light wavelength for optimizing microscopic signal to noise resolution that is also based on pinhole diameter and magnification, using a Zeiss 710 Confocal Laser Microscope maintained by Virginia Commonwealth University.
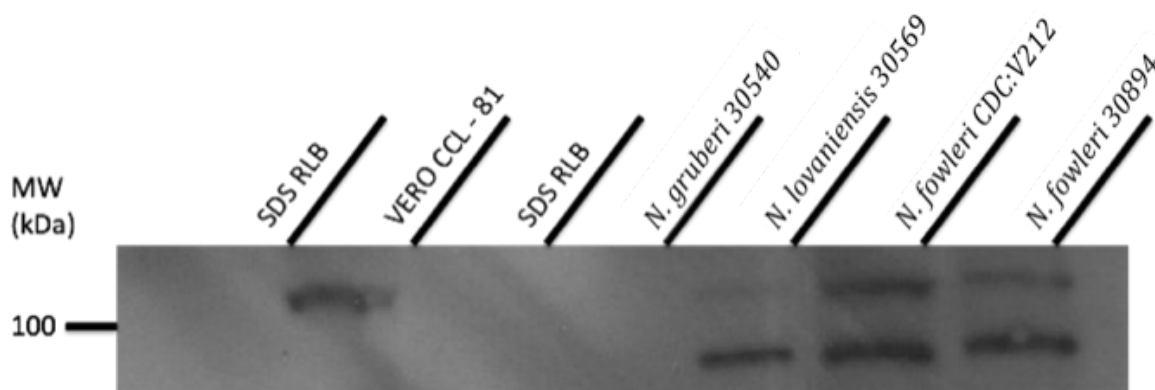
Results

Figure 1. Western immunoblotting of an Novex™ WedgeWell™ 8% Tris-Glycine Gel transferred to nitrocellulose after loading with 50 μg of whole-cell lysates of *N. fowleri* CDC:V212, *N. fowleri* 30894, *N. gruberi* 30540, and *N. lovaniensis* 30569 and a eukaryotic cell control, including Vero CCL-81, in their respective lanes, probed with 1:1000 of polyclonal anti-beta-COPI Rabbit IgG overnight with expression at the predicted 110 kDa for the beta-COPI subunit in Vero CCL-81, *N. lovaniensis* 30569, *N. fowleri* CDC:V212, and *N. fowleri* 30894. Three independent experiments were performed.
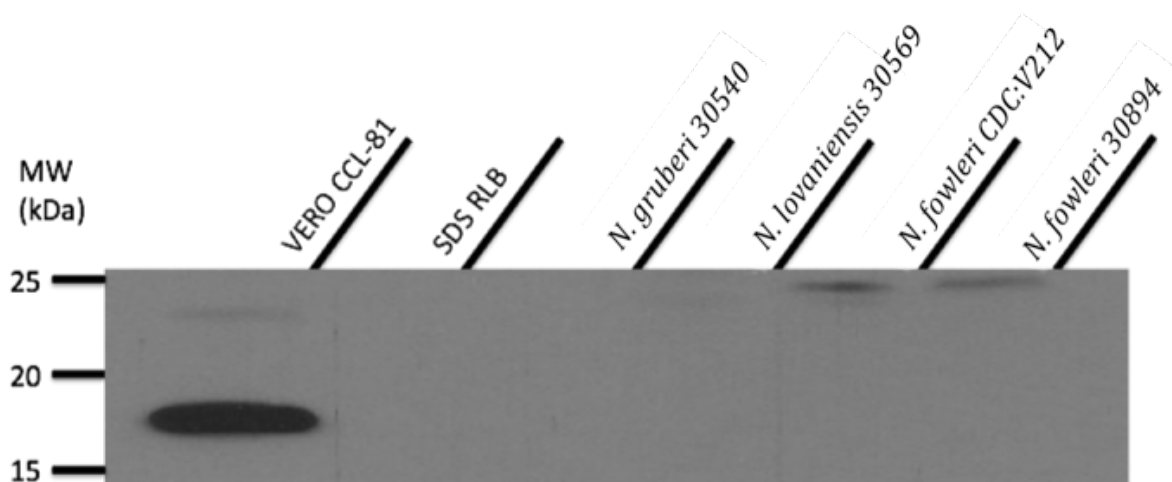

Figure 2. Western immunoblotting of a Novex™ WedgeWell™ 12% Tris-Glycine Gel transferred to nitrocellulose after loading with 25 μg of whole-cell lysates of respective amoebae and a

eukaryotic control, including Vero CCL-81, *N. fowleri* CDC:V212, *N. fowleri* 30894, *N. gruberi*

30540, and *N. lovaniensis* 30569 in their respective lanes, probed with 1:1000 of polyclonal Arf1

anti-Rabbit IgG showing expression at the predicted 18 kDa for Arf1 in Vero CCL-81 and

possible post-translationally modified Arf1 in *N. lovaniensis* 30569, *N. fowleri* CDC:V212, and *N.*

fowleri 30894. Three independent experiments were performed.
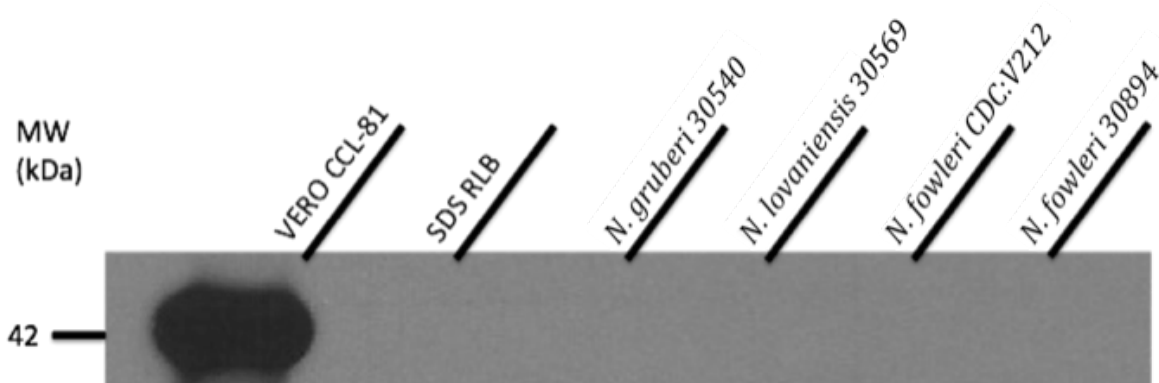
Figure 3. Western immunoblotting of an Novex™ WedgeWell™ 12% Tris-Glycine transferred to

nitrocellulose after loading with 50 µg of whole-cell lysates of respective amoebae and a

eukaryotic control, including Vero CCL-81, *N. fowleri* CDC:V212, *N. fowleri* 30894, *N. gruberi*

30540, and *N. lovaniensis* 30569 in their respective lanes, probed with 1:1000 of polyclonal anti-

beta-actin Rabbit IgG showing expression at the predicted 41 kDa for the beta-actin subunit in

Vero CCL-81 but not *N. lovaniensis* 30569, *N. fowleri* CDC:V212, and *N. fowleri* 30894. Three

independent experiments were performed.

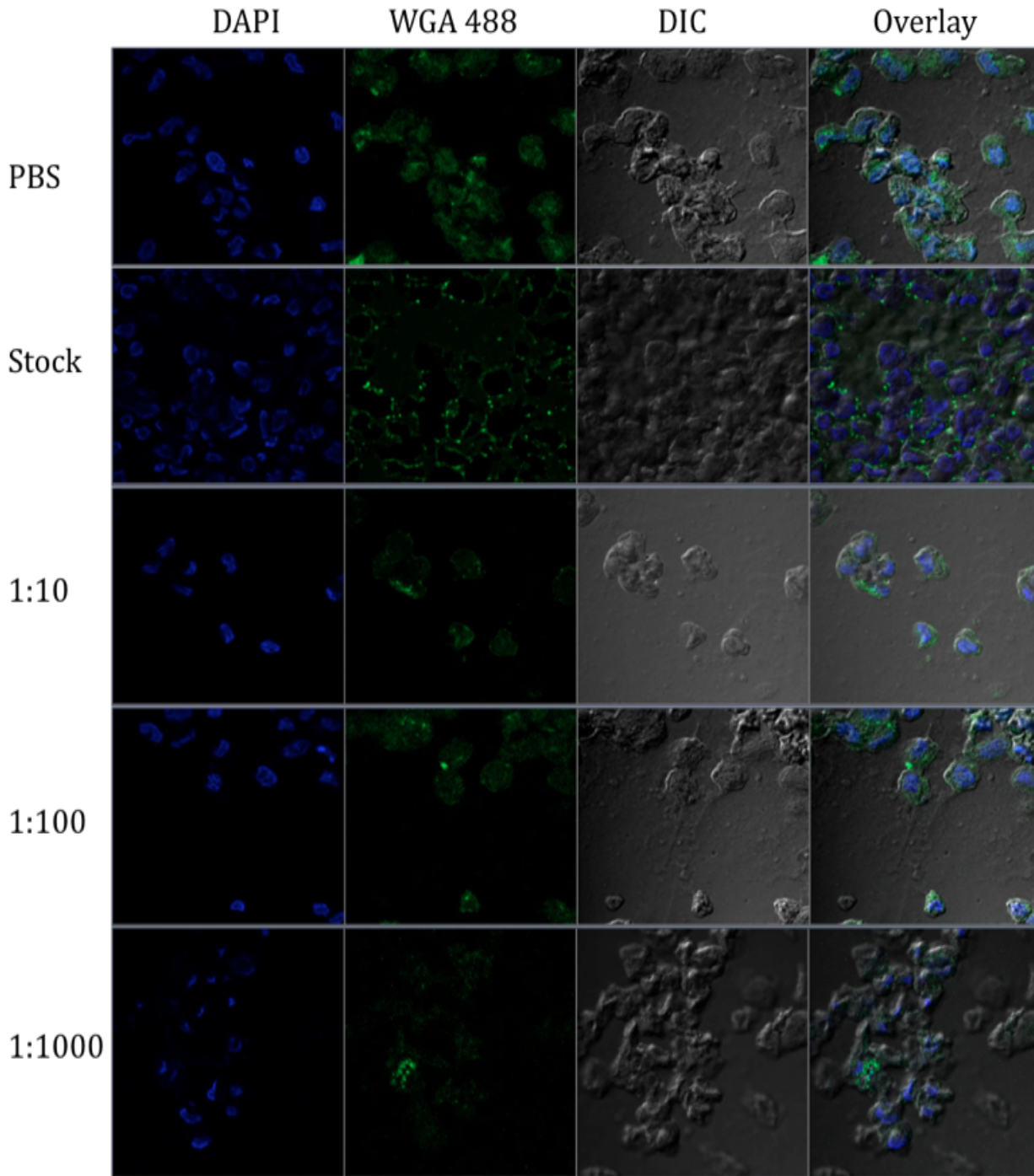Figure 4. Confocal micrographs consisting of 2% paraformaldehyde, heat-fixed Vero CCL-81 cells incubated with varying serial dilutions of Wheat Germ Agglutinin Alexa Fluor 488, a trans-Golgi marker, starting with the recommended stock solution (5 µg/mL) and decreasing ten-fold per dilution in each respective row. From left to right, DAPI, WGA 488, differential interface contrast,

and their respective overlays were captured of each representative slide. For mounting,

Vectashield with DAPI was utilized. Pixel size was adjusted to 0.09 μm and the primary

wavelength coordinating with WGA 488 and adjusted to 1 Airy Unit (1 AU). All images viewed at

63X on the Zeiss Laser Scanning Microscope 710 maintained by Virginia Commonwealth

University. Experiments performed three times independently in duplicates with best

representative images selected.

Figure 5. Confocal micrographs consisting of 2% paraformaldehyde, heat-fixed *N. fowleri* 30894

cells incubated with varying serial dilutions of Wheat Germ Agglutinin 488, a trans-Golgi marker,

starting with the recommended stock solution (5 µg/mL) and decreasing ten-fold per dilution in

each respective row. From left to right columns, DAPI, WGA 488, differential interface contrast,

and their respective overlays were captured of each representative slide. For mounting,

Vectashield with DAPI was utilized. Pixel size was adjusted to 0.09 µm and the primary

wavelength coordinating with WGA 488 and adjusted to 1 Airy Unit (1 AU). All images viewed at

63X on the Zeiss Laser Scanning Microscope 710 maintained by Virginia Commonwealth

University. Experiments performed three times independently in duplicates with best
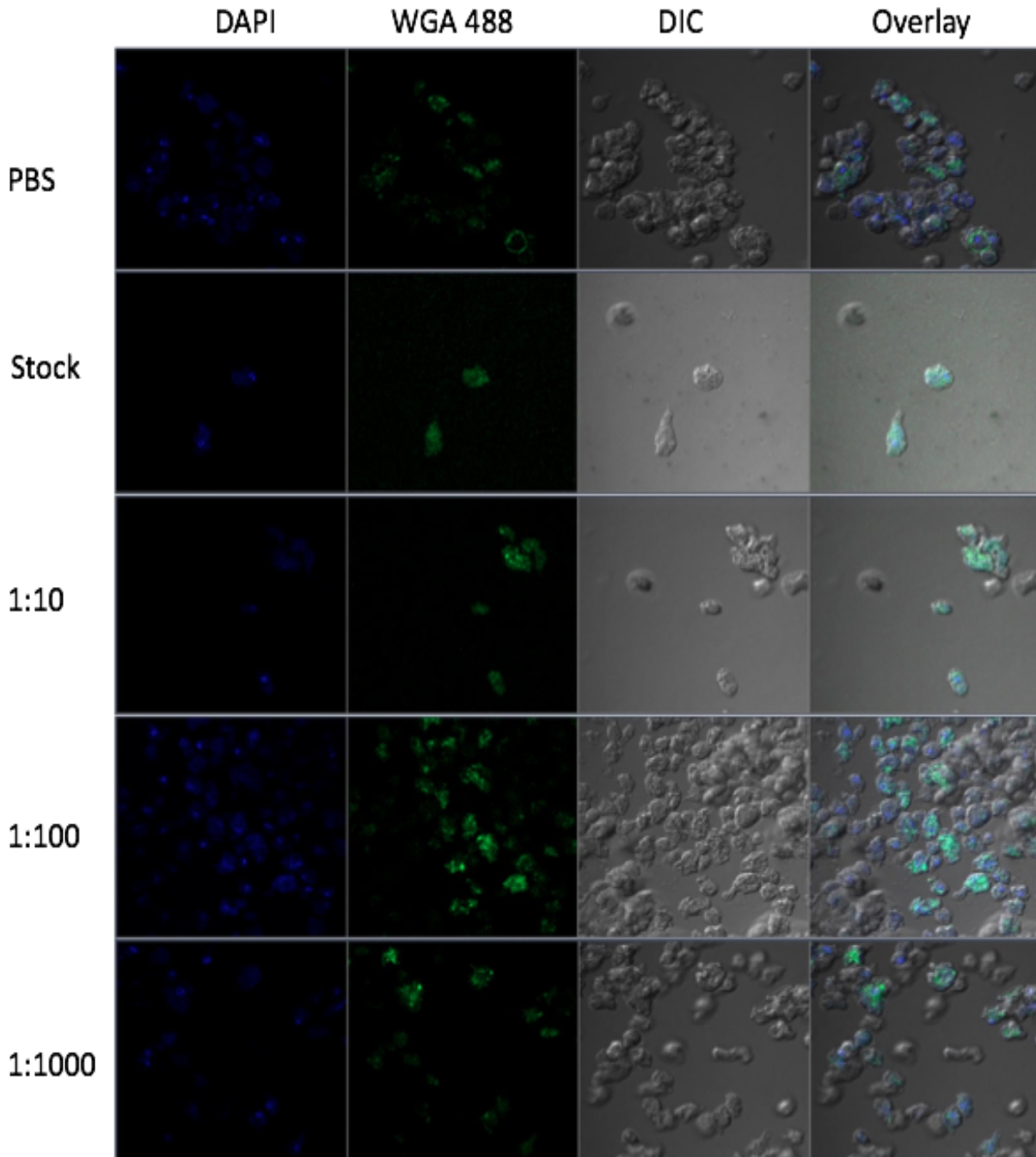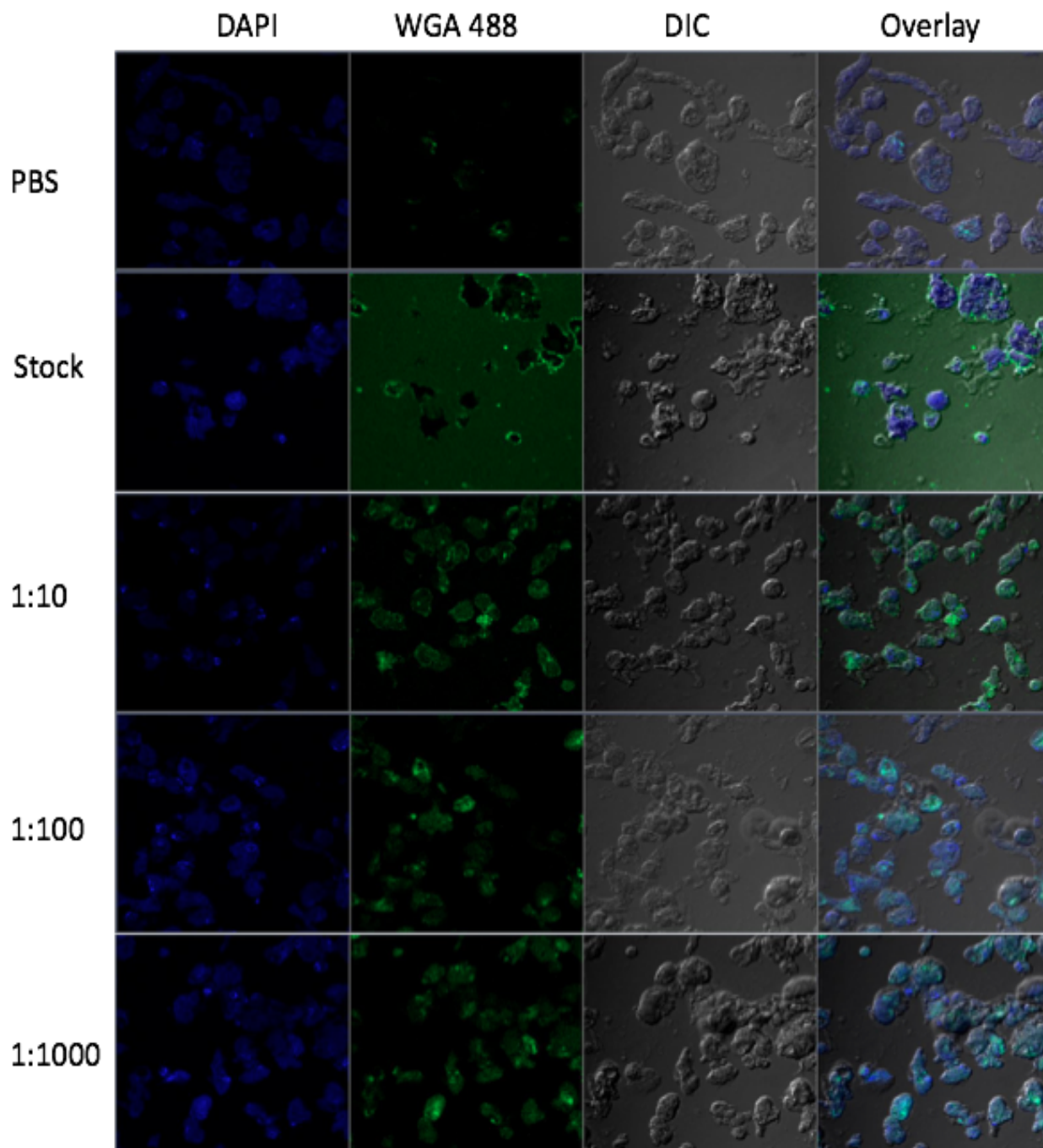
representative images selected.

Figure 6. Confocal micrographs consisting of 2% paraformaldehyde, heat-fixed *N. gruberi* 30540 cells incubated with varying serial dilutions of Wheat Germ Agglutinin 488, a trans-Golgi marker, starting with the recommended stock solution (5 μg/mL) and decreasing ten-fold per dilution in each respective row. From left to right columns, DAPI, WGA 488, differential interface contrast, and their respective overlays were captured of each representative slide. For mounting, Vectashield with DAPI was utilized. Pixel size was adjusted to 0.09 μm and the primary wavelength coordinating with WGA 488 and adjusted to 1 Airy Unit (1 AU). All images viewed at 63X on the Zeiss Laser Scanning Microscope 710 maintained by Virginia Commonwealth University. Experiments performed three times independently in duplicates with best representative images selected.

Figure 7. Sequential immunofluorescence micrographs of 2% paraformaldehyde, heat-fixed Vero CCL-81 cells assessed for the presence of a Golgi apparatus by probing with 1:100 WGA 488, a trans-Golgi marker, for 10 minutes and then probed with 1:250 beta-COPI, a cis-Golgi marker, for 1 hour for the bottom row while 1:250 of 3% BSA:PBS was utilized in the top control row. Subsequent incubation with 1:1000 Alexa Fluor 594 followed; rows labeled "1:1000" had no

primary antibody administered to the sample, only WGA 488 and Alexa Fluor 594 and considered the negative control for beta-COPI. For mounting, Vectashield with DAPI was utilized. Pixel size was adjusted to 0.09 μm, and the median wavelength, coordinating with WGA 488, adjusted to 1 Airy Unit (1 AU). All images viewed and collected at 63X on the Zeiss Laser Scanning Microscope 710 maintained by Virginia Commonwealth University. Experiments performed three times independently in duplicates with best representative images selected.
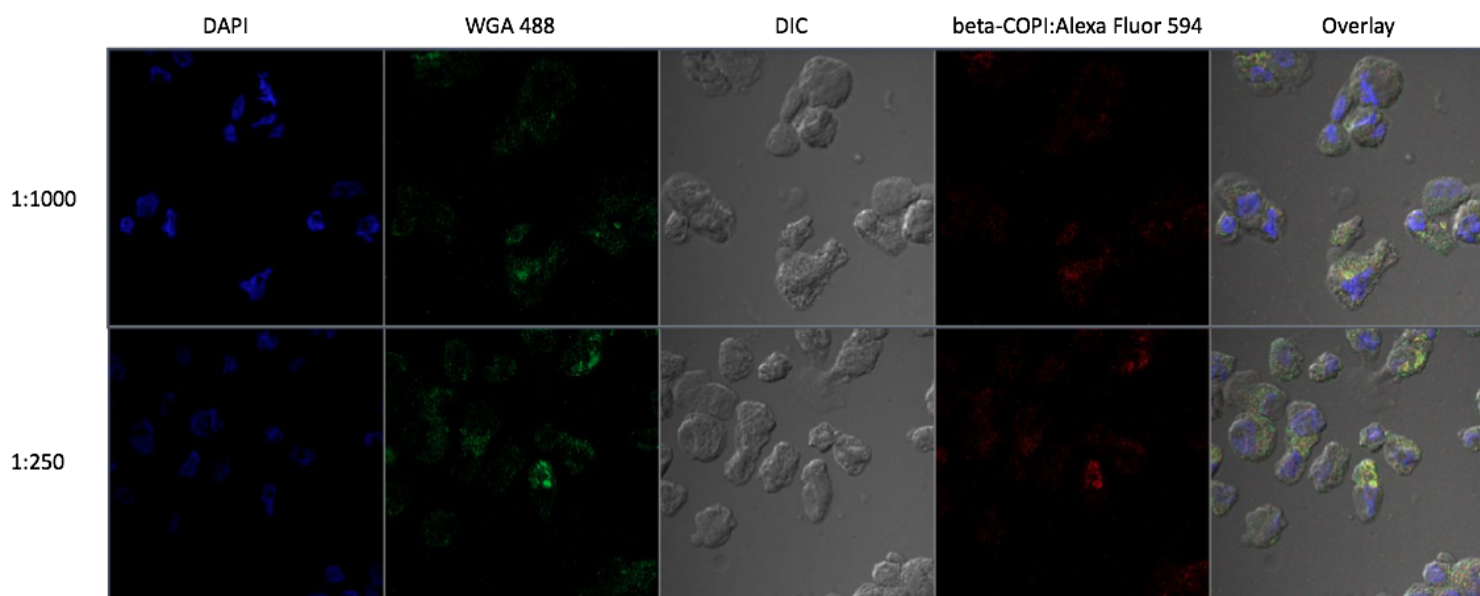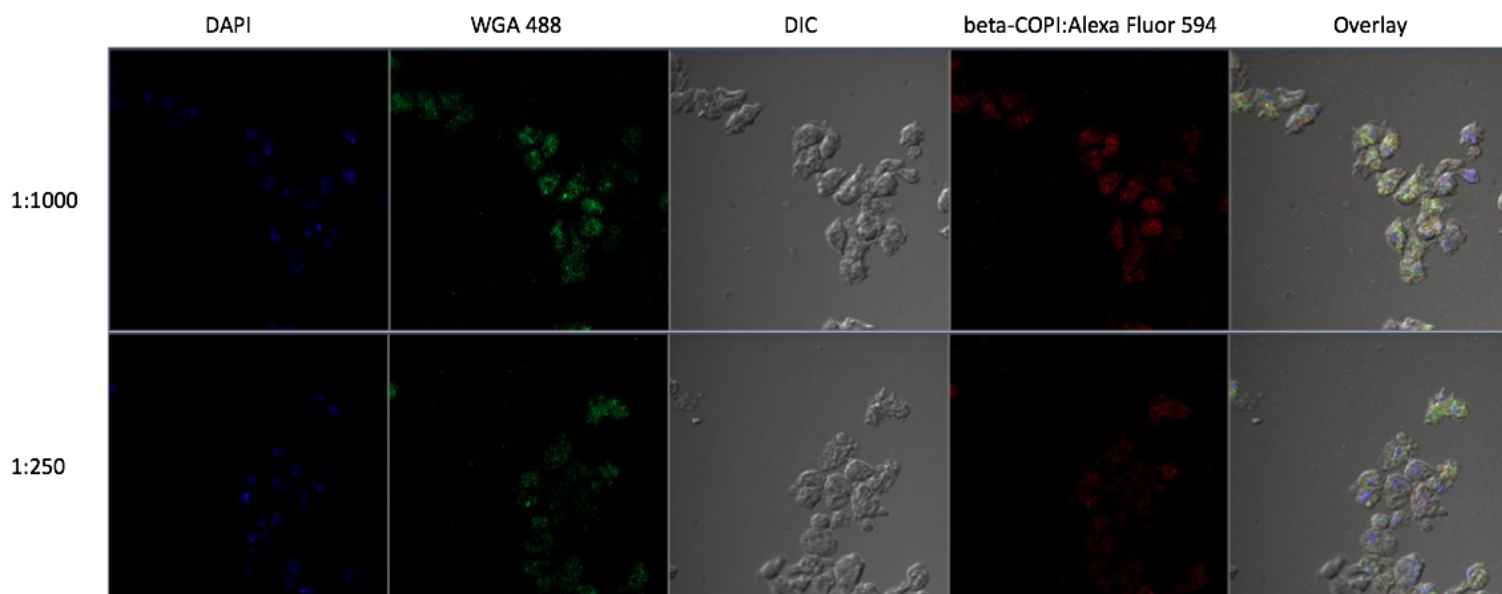

Figure 8. Sequential immunofluorescence micrographs of 2% paraformaldehyde, heat-fixed *N. fowleri* 30894 cells assessed for the presence of a Golgi apparatus by probing with 1:100 WGA 488, a trans-Golgi marker, for 10 minutes and then probed with 1:250 beta-COPI, a cis-Golgi marker, for 1 hour for the bottom row while 1:250 of 3% BSA:PBS was utilized in the top control row. Subsequent incubation with 1:1000 Alexa Fluor 594 followed; rows labeled "1:1000" had no primary antibody administered to the sample, only WGA 488 and Alexa Fluor 594 and considered the negative control for beta-COPI. For mounting, Vectashield with DAPI was utilized. Pixel size

was adjusted to 0.09 µm, and the median wavelength, coordinating with WGA 488, adjusted to 1

Airy Unit (1 AU). All images viewed at 63X on the Zeiss Laser Scanning Microscope 710

maintained by Virginia Commonwealth University. Experiments performed three times

independently in duplicates with best representative images selected.

Figure 9. Sequential immunofluorescence micrographs of 2% paraformaldehyde, heat-fixed *N.*

fowleri 30894 cells in division showing vesicle trafficking from dispersed Golgi bodies assessed

for the presence of a Golgi apparatus by probing with 1:100 WGA 488, a trans-Golgi marker, for

10 minutes and then probed with 1:250 beta-COPI, a cis-Golgi marker, for 1 hour with 1:1000

Alexa Fluor 594 following; For mounting, Vectashield with DAPI was utilized. Pixel size was

adjusted to 0.09 µm, and the median wavelength, coordinating with WGA 488, adjusted to 1 Airy

Unit (1 AU). All images viewed at 63X on the Zeiss Laser Scanning Microscope 710 maintained

by Virginia Commonwealth University. Experiments performed three times independently in

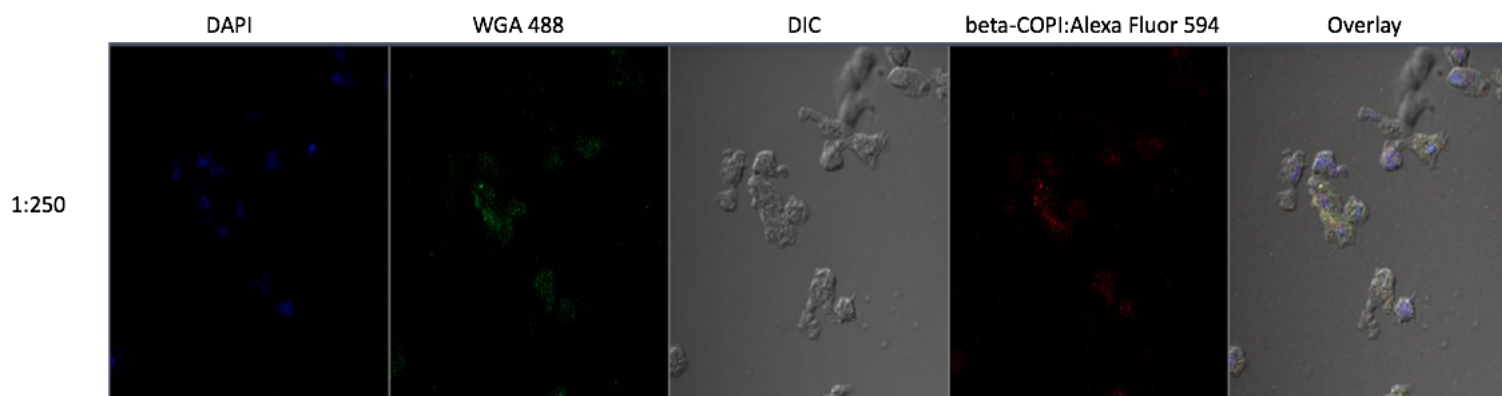duplicates with best representative images selected.

To determine the presence or absence of classically conserved eukaryotic Golgi proteins, western immunoblots of whole-cell lysates of axenically grown *N. fowleri* CDC:V212, *N. fowleri* 30894, *N. gruberi* 30540, and *N. lovaniensis* 30569 were performed while utilizing Vero CCL-81 cells as a positive control. Rabbit polyclonal IgG antibodies generated against the beta-COPI subunit and ARF1 were utilized to screen for the presence of expressed but reduced proteins of amebic whole-cell lysates. Western blot of whole-cell lysates at 50 µg against the beta-COPI subunit showed the presence of reduced protein bands at 110 kDa in whole-cell lysates of Vero CCL-81, *N. lovaniensis* 30569, *N. fowleri* CDC:V212, and *N. fowleri* 30894 with absence in N. gruberi 30540 and the SDS-reducing lysate negative control lanes (Figure 1). Western blot of whole-cell lysates against the ARF1 subunit showed the presence of bands at 18 kDa in whole-cell lysates of Vero CCL-81 and weak bands near 25 kDa for Vero CCL-81, *N. lovaniensis* 30569, *N. fowleri* CDC:V212, and *N. fowleri* 30894 with absence in *N. gruberi* 30540 and the SDS-reducing lysate negative control lanes with wells loaded at 25 µg (Figure 2). Western immunoblots of whole-cell lysates against the beta-actin with rabbit polyclonal IgG for loading controls showed the presence of bands at 42 kDa in whole-cell lysates of Vero CCL-81 but not in *N. lovaniensis* 30569, *N. fowleri* CDC:V212, N. *fowleri* 30894, and *N. gruberi* 30540 and no bands indicating binding to reduced proteins present in the SDS-reducing lysate negative control lanes with wells loaded at 50 µg (Figure 3).

A WGA 488 study conducted by Model *et al* in 2012 determined that WGA 488 Alexa Fluor could be calibrated and linearly expressed in many cell lines with reproducibility at 97%, indicating that with proper dilution technique could offer a consistent application of soluble WGA 488, a trans-Golgi marker (Chazotte, 2011). With this purpose in mind, heat-fixed Vero cells, *N. fowleri* 30894, and *N. gruberi* 30540 were utilized for this process. Vero cells showed high background and binding to the outer membrane leaflet with the recommended stock dilution of WGA 488 with nonspecific autofluorescence of Vero cells in PBS (Figure 4). Decreased binding

of WGA 488 occurred in serial dilutions of WGA 488 with Golgi apparatus indications nearby the

DAPI stained nuclei in 1:10 and 1:100 dilutions, with a lower resolution of Golgi presence at

1:1000 (Figure 4). *N. fowleri* 30894 cells showed high background and binding to the outer

membrane leaflet with the recommended stock dilution (5 µg/mL) of WGA 488 with nonspecific

autofluorescence of *N. fowleri* 30894 cells in 1X PBS (Figure 5). Dispersed bodies bound near

the nucleus appear around 1:10 and 1:100 dilutions in *N. fowleri* 30894 with reduction of

presence in 1:1000 unless cells are in division (Figure 5). *N. gruberi* 30540 cells showed a high

background of WGA 488 and binding to the outer membrane leaflet with the recommended

stock dilution of WGA 488 with little autofluorescence of *N. gruberi* 30540 cells in 1X PBS and

high DAPI permeation throughout the cells. At 1:10 dilution, signal to noise ratio was equalized

and tubular structures could be seen in *N. gruberi* 30540 cells (Figure 6). 1:100 and 1:1000

dilutions of stock WGA 488 had DAPI permeation and decreased distinction of Golgi tubules in

N. gruberi 30540 cells (Figure 6).

To deduce the presence of a Golgi in polymorphic amoeba, nonspecific labeling with

WGA 488, a trans-Golgi marker, was utilized to distinguish between the presence of a

concerted Golgi apparatus in Vero cells and the possible expression and presence of a Golgi in

ameba. Serial dilutions were utilized to determine the appropriate range of WGA 488 Alexa

Fluor for sequential beta-COPI, a cis-Golgi marker, immunofluorescence with recognition of

1:100 being most appropriate for the next sequential assay. The secondary antibody was

distributed alone without primary antibody specificity to confirm immunofluorescence results and

nonspecific binding. Vero CCL-81 cells showed decreased binding with 1:1000 Alexa Fluor 594

applied without the primary beta-COPI antibody (Figure 7). WGA 488 binding in Vero CCL-81

cells were consistent with the 1:100 distribution in the previous assay, with binding to the

cytosolic proteins and apparent trans-Golgi apparatus features near the nucleus (Figure 4,

Figure 7). Vero CCL-81 cells showed binding to cis-Golgi apparatus with the application of

primary 1:250 beta-COPI and 1:1000 Alexa Fluor 594 closer to the nucleus than WGA 488

binding presence (Figure 7).

The opposite expression of nonspecific binding occurred in *N. fowleri* 30894 with 1:1000

Alexa Fluor 594 applied without the primary beta-COPI antibody, with a wide range of overlap

(Figure 8). WGA 488 binding in *N. fowleri* cells were consistent with the 1:100 distribution in the

previous assay, showing dispersed bodies bound in the cytoplasm (Figure 5, Figure 8). *N.*

fowleri cells showed binding to a possible cis-Golgi apparatus with the application of primary

1:250 beta-COPI and 1:1000 Alexa Fluor 594 closer to the nucleus than WGA 488 presence

that typically indicates the trans-Golgi network complex (Figure 8). Presence of Golgi bodies

migrating to another nucleus in dividing *N. fowleri* can be seen in Figure 9 overlayed with the

application of primary 1:250 beta-COPI and 1:1000 Alexa Fluor 594 closer to the nucleus than

WGA 488 with coexpression and colocalization in mitotic cells.

Discussion

       The Golgi apparatus has the potential for polymorphic expression based on a variety of studies and can utilize different functional forms, such as dispersed cisternae in *Saccharomyces cerevisiae* or multiple compartmental Golgi apparatuses such as those found within *Pichia pistoris* (Suda and Nakano, 2012). *Entamoeba histolytica* and *Mastigamoeba balamuthi* lack identifiable stacked Golgi apparatuses and have been shown to be dispersed in Golgi studies for *M. balamuthi* and punctate Golgi bodies respectively in *E. histolytica* (Ghosh *et al.,* 1999; Barlow *et al.*, 2018) While Herman *et al.* 2018 found the Golgi apparatus as dispersed tubule structures in *N. gruberi* and while *N. fowleri* was determined to have functional orthologues of Golgi machinery based on *in silico* predictions, *N. fowleri* is considered more closely related to *N. lovaniensis* than *N. gruberi* (Liechti *et al*., 2018). This allows for the possibility of *Naegleria fowleri* having different expression in the morphology of the Golgi apparatus that is possible with distinct evolutionary divergence, with the possibility of orthologous molecular conservation (Herman *et al.,* 2018).

       Entamoeba histolytica does not have typical Eukaryotic mitotic phasic checkpoints, which opens the possibility that *N. fowleri* could have a potential to lack these checkpoints (Banerjee *et al.* 2002; Barlow *et al*., 2018). A review study suggests that stacking functions in the Golgi retain themselves in transport and conversion to mitotic vesicles, potentially confirming the coexpression of WGA 488 as a trans-Golgi marker with a beta-COPI, a cis-Golgi vesicles marker, in Figure 9 (Warren, 1993). When utilizing cis-Golgi and trans-Golgi markers, *N. fowleri* can be examined to have vesicles in close proximity in division and in normal cell polymorphisms, promoting the punctate, organized but dispersed Golgi bodies, which would be efficient in polymorphic amoeba for movement and displacement of proteins for pseudopodia creation via actin formation and degradation (Figure 8 and 9) (Zysset-Burri *et al.*, 2014).

       Western immunoblotting is a powerful technique that can be utilized to show the expressed proteins within a cell or species. However, this expression is dependant on the

primary antibody avidity to the sequence within the samples of whole-cell lysates or membrane fractions, which have the potential for limited binding or nonspecific binding under varying conditions. Although a powerful technique, Western immunoblotting can be potentially problematic due to electrostatically-like charge repulsion on nitrocellulose and need for specified loading controls with species variations, such a beta-actin IgG generated against *Naegleria* sp. as a Eukaryotic loading control (Low *et al*., 2013; Bass *et al*., 2016; Kim *et al*., 2016). Commercially available antibodies for loading controls of beta-actin do not typically react with reduced proteins in whole-cell lysates of *Naegleria* species as several commercially available anti-beta-actin polyclonal rabbit antibodies and mouse monoclonal antibodies were utilized without consistent results for Western immunoblotting (Figure 3), which could be due to concerted actin proteases not inhibited by the anti-proteases in the Roche^{TM} mammalian cocktail being not species-specific enough within the whole-cell lysates of *Naegleria* species. A more likely scenario of mammalian antibodies being not species-specific enough for *Naegleria* sp. beta-actin were the result (Sohn *et al.*, 2010; Zyserman *et al.,* 2018). Beta-COPI and ARF1 and preliminary data on the alpha-COPI subunit, with subsequent 140 kDa band association (data not shown), have been shown to be conserved in *Naegleria* sp., such as *N. fowleri* and *N. lovaniensis*, with the utilization of commercially available rabbit polyclonal IgG antibodies (Figure 1 and 2). With such distinct banding patterns in *N. fowleri* and *N. lovaniensis* with beta-COPI, it could prove useful as a diagnostic tool for infection if amoeba can be cultured early enough and Western immunoblots are performed within a short time period for patients with an indication of PAM and/or amebic infection (Figure 1).

Wheat Germ Agglutinin Alexa Fluor^{TM} 488 binds to N-acetyl-D-glucosamine residues and sialic acids and act as potential trans-Golgi vesicles markers in fixed cells stained with WGA. WGA was shown to be more consistent with reliable binding than other conjugated lectins, allowing for potentially near-linear reproducibility, particularly with lower dilutions, which was found based on gray level and this knowledge could potentially be helpful in future studies

of WGA assays such as those found in Figures 4, 5, and 6 (Wang *et al*., 2010; Chazotte, 2011).

Triton X-100 disrupts membranes and glycosyltransferase of the Golgi, which can cause

potential impact in cell signaling and structural and storage changes (Breton *et al.,* 2006;

Fleischer, 1981) Lipid rafts are potentially removed with Triton X-100 and this causes migration

to the outer membrane of the cell and dispersion within 15 minutes of Triton X-100 0.1%

[vol/vol] and was shown to cause this effect via atomic force microscopy, which is why Triton X-

100 was not utilized in this study (Xu *et al.*, 2013; Alonso and Millan, 2001). A study in 2017

concluded that paraformaldehyde coupled with methanol was optimal for immunofluorescence,

which was utilized in this study in Figures 7, 8, and 9 for sequential immunofluorescence (Yuan

et al., 2017). Immunofluorescence has changed over the years and no longer requires the use

of BSA, according to Buchwalow *et al*., 2011. BSA also contains native tryptophan residues,

which can possibly impact immunofluorescence with a redshift when utilized as a blocking agent

and coupled with the wrong antibodies, or possibly have nonspecific binding in cells grown in

fetal calf serum, and this knowledge can be potentially problematic in cytosolic products with

high tryptophan residues in protein sequences, possibly explaining the background in Figure 8

in the control group (Vivian and Callis, 2001; Buchwalow *et al*., 2011; Chib *et al.*, 2015). Further

study of the internal Stark effect on amoeba could prove useful for future studies in

immunofluorescence.

      PAM is an efficient and subversive infection presenting signs and symptoms of a typical

infection but resulting in a 97% mortality in the past 100 cases, so learning the morphology and

molecular processes should be paramount before using a drug regime that could select for

resilient strains as the amoeba can still have the potential to survive the host's death with the

cyst stage (Marciano-Cabral *et al*., 2007). Drugs for treatment should also be used in tandem

with other molecular inhibitory pharmaceuticals or techniques, such as artificial hypothermia

induction while maximizing minimum patient harm and mitigated drug side-effects (Eddy *et al*.,

2009). In this study, the Golgi apparatus was determined to have strong indications of

colocalization with cis-Golgi and trans-Golgi molecules in *Naegleria fowleri* 30894 in dividing amoeba and non-dividing amoeba and Vero cells, a positive mammalian control (Figure 7, 8, and 9). Time-lapse studies on division would be optimal for future studies due to the intrinsic bias of assuming mitosis is conserved and that many studies fix organisms rather than using live-cell staining, which is particularly true with amebic evolutionary divergence from Eukaryotic cells over a billion years ago (González-Robles *et al.,* 2009; Fritz-Laylin *et al*., 2010).

Future directions of study confirming molecular expression via genetic analysis would greatly improve the ability to produce antibodies generated specifically toward *Naegleria fowleri* protein sequences of beta-COPI as a cis-Golgi marker. Diverse carbohydrate residues should also be taken into account for *Naegleria* sp. and for the utilization of lectins (González-Robles *et al*., 2007). Brefeldin A can be utilized to confirm Golgi expression, but ARF1 presence and other molecular interactions determined via genetic studies should be confirmed before its use to prevent artificial confirmation based on observational changes of vesicle disruption, especially when multiple domains of vesicle trafficking can be disturbed by Brefeldin A, and most Golgi trafficking typically relies on studies based on expressed mammalian Golgi and microtubules, whereas *N. gruberi* and other amoebae do not contain nor rely on microtubules in the amoebic stage and with the knowledge that the fungal metabolite, Brefeldin A, can have different species interactions (Pelham, 1991; Chardin and McCormick*,* 1999; Zeeh *et al*., 2006; Fritz-Laylin *et al*., 2010; Herman *et al*., 2018).

References

Alonso, M. A., & Millán, J. (2001). The role of lipid rafts in signaling and membrane trafficking in T lymphocytes. *Journal of Cell Science*, *114*(Pt 22), 3957–3965. Retrieved from http://www.ncbi.nlm.nih.gov/pubmed/11739628

Banerjee, S., Das, S., & Lohia, A. (2002). Eukaryotic checkpoints are absent in the cell division cycle of Entamoeba histolytica. *Journal of Biosciences*, *27*(6 SUPPL. 3), 567–572. Retrieved from https://doi.org/10.1007/BF02704849

Barlow, L. D., Nývltová, E., Aguilar, M., Tachezy, J., & Dacks, J. B. (2018). A sophisticated, differentiated Golgi in the ancestor of eukaryotes. *BMC Biology*, *16*(27), 1–15. Retrieved from https://www.ncbi.nlm.nih.gov/pmc/articles/PMC5840792/pdf/12915_2018_Article_492.pdf

Bass, J. J., Wilkinson, D. J., Rankin, D., Phillips, B. E., Szewczyk, N. J., Smith, K., & Atherton, P. J. (2017). An overview of technical considerations for Western blotting applications to physiological research. *Scandinavian Journal of Medicine and Science in Sports*, *27*(1), 4–25. Retrieved from https://doi.org/10.1111/sms.12702

Bradford, M.M. (1976). A rapid and sensitive method for the quantitation of microgram quantities of protein utilizing the principle of protein-dye binding. Anal Biochem: 72(1–2): 248–254.

Breton, C., Šnajdrová, L., Jeanneau, C., Koča, J., & Imberty, A. (2006). Structures and mechanisms of glycosyltransferases. *Glycobiology*, *16*(2), 29–37. Retrieved from https://doi.org/10.1093/glycob/cwj016

Buchwalow, I., Samoilova, V., Boecker, W., & Tiemann, M. (2011). Non-specific binding of antibodies in immunohistochemistry: Fallacies and facts. Scientific Reports, 1, 1–6. Retrieved from https://doi.org/10.1038/srep00028

Chardin, P., & Mccormick, F. (1999). Brefeldin A: The Advantage Minireview of Being
    Uncompetitive of brefeldin A action might have important implications for drug
    discovery. By what mechanism does brefeldin A inhibit Arf1 ex- the characterization of
    the mutations in brefeldin A–resistant mut. *Cell*, *97*, 153–155. Retrieved from
    http://www.cell.com/cell/pdf/S0092-8674(00)80724-2.pdf

Chazotte, B. (2011). Labeling membrane glycoproteins or glycolipids with fluorescent
    wheat germ agglutinin. *Cold Spring Harbor Protocols*, *6*(5), 570–573. Retrieved from
    https://doi.org/10.1101/pdb.prot5623

Chib, R., Butler, S., Raut, S., Shah, S., Borejdo, J., Gryczynski, Z., and Gryczynski, I.
    Effect of Quencher, Denaturants,Temperature and pH on the Fluorescent Properties
    of BSA Protected Gold Nanoclusters. J Lumin. 2015; 168: 62–68. Retrieved from
    https://doi.org/10.1016/j.jlumin.2015.07.030

Cope, J. R., & Ali, I. K. (2016). Primary Amebic Meningoencephalitis: What Have We
    Learned in the Last 5 Years? *Current Infectious Disease Reports*, *18*(10), 1–11.
    Retrieved from https://doi.org/10.1007/s11908-016-0539-4

Eddy, B. A., Capewll, L., Yoder, J. S., Beach, M. J., & Visvesvara, G. S. (2009). The
    epidemiology of primary amoebic meningoencephalitis in the USA, 1962–2008.
    Epidemiology and Infection, *138*(07), 968–975. Retrieved from
    https://doi.org/10.1017/s0950268809991014

Marciano-Cabral, F.M., Patterson, M., John, D.T., and Bradley, S.Q. (1982).
    Cytopathogenicity of Naegleria fowleri and Naegleria gruberi for Established
    Mammalian Cell Cultures. *The Journal of Parasitology*, *68*(6), 1110–1116. Retrieved
    from https://www.jstor.org/stable/3281100

Fleischer, B. (1981). Orientation of glycoprotein galactosyltransferase and sialyltransferase
    enzymes in vesicles derived from rat liver Golgi apparatus. *Journal of Cell Biology*,
    89(2), 246–255. Retrieved from https://doi.org/10.1083/jcb.89.2.246

Fritz-Laylin, L. K., Assaf, Z. J., Chen, S., & Cande, W. Z. (2010). Naegleria gruberi De

    Novo Basal Body Assembly Occurs via Stepwise Incorporation of Conserved

    Proteins. *Eukaryotic Cell*, *9*(6), 860–865. Retrieved from

    https://doi.org/10.1128/ec.00381-09

Fritz-Laylin, L. K., Prochnik, S. E., Ginger, M. L., Dacks, J. B., Carpenter, M. L., Field, M.

    C., … Dawson, S. C. (2010). The Genome of Naegleria gruberi Illuminates Early

    Eukaryotic Versatility. *Cell*, *140*(5), 631–642. Retrieved from

    https://doi.org/10.1016/j.cell.2010.01.032

Ghosh, S. K., Field, J., Frisardi, M., Rosenthal, B., Mai, Z., Rogers, R., & Samuelson, J.

    (1999). Chitinase secretion by encysting Entamoeba invadens and transfected

    Entamoeba histolytica trophozoites: Localization of secretory vesicles, endoplasmic

    reticulum, and Golgi apparatus. *Infection and Immunity*, *67*(6), 3073–3081.

González-Robles, A., Cristóbal-Ramos, A. R., González-Lázaro, M., Omaña-Molina, M., &

    Martínez-Palomo, A. (2009). Naegleria fowleri: Light and electron microscopy study of

    mitosis. *Experimental Parasitology*, *122*(3), 212–217. Retrieved from

    https://doi.org/10.1016/j.exppara.2009.03.016

González-Robles, A., Castañón, G., Cristóbal-Ramos, A. R., Hernández-Ramírez, V. I.,

    Omaña-Molina, M., & Martínez-Palomo, A. (2007). Cell surface differences of

    Naegleria fowleri and Naegleria lovaniensis exposed with surface markers.

    Experimental Parasitology, *117*(4), 399–404. Retrieved from

    https://doi.org/10.1016/j.exppara.2007.05.007

Herman, E. K., Yiangou, L., Cantoni, D. M., Miller, C. N., Marciano-Cabral, F.,

    Anthonyrajah, E., … Tsaousis, A. D. (2018). Identification and characterisation of a

    cryptic Golgi complex in *Naegleria gruberi*. *Journal of Cell Science*, *131*(7), jcs213306.

    Retrieved from https://doi.org/10.1242/jcs.213306

Hunte, T., Morris, T., da Silva, A., & Al, E. (2013). Primary Amebic Meningoencephalitis

    Associated with Ritual Nasal Rinsing — St. Thomas, U.S. Virgin Islands, 2012 On.

    Morbidity and Mortality Weekly Report, *62*(45), 903. Retrieved from

    http://www.cdc.gov/mmwr/pdf/wk/mm6245.pdf

Jamerson, M., da Rocha-Azevedo, B., Cabral, G. A., & Marciano-Cabral, F. (2012).

    Pathogenic Naegleria fowleri and non-pathogenic Naegleria lovaniensis exhibit

    differential adhesion to, and invasion of extracellular matrix proteins. *Microbiology*,

    158(3), 791–803. Retrieved from https://doi.org/10.1099/mic.0.055020-0

Jayaram, S. A., Senti, K. A., Tiklová, K., Tsarouhas, V., Hemphälä, J., & Samakovlis, C.

    (2008). COPI vesicle transport is a common requirement for tube expansion in

    Drosophila. *PLoS ONE*, *3*(4). Retrieved from

    https://doi.org/10.1371/journal.pone.0001964

Kim, J.-H., Sohn, H.-J., Yoo, J.-K., Kang, H., Seong, G.-S., Chwae, Y.-J., … Shin, H.-J.

    (2016). NLRP3 Inflammasome Activation in THP-1 Target Cells Triggered by

    Pathogenic Naegleria fowleri. *Infection and Immunity*, *84*(9), 2422–2428. Retrieved

    from https://doi.org/10.1128/iai.00275-16

Kruger, N. J. (1996). The Bradford Method From: The Protein Protocols Handbook, 2nd

    Edition The Bradford Method for Protein Quantitation. *The Protein Protocols*

    Handbook, 15–20. Retrieved from https://doi.org/10.1007/978-1-60327-259-9_4

Liechti, N., Schürch, N., Bruggmann, R., & Wittwer, M. (2018). The genome of Naegleria

    lovaniensis, the basis for a comparative approach to unravel pathogenicity factors of

    the human pathogenic amoeba N. fowleri. *BMC Genomics*, *19*(1), 1–11. Retrieved

    from https://doi.org/10.1186/s12864-018-4994-1

Lodish, H., Berk, A., Zipursky, S.L., et al. Molecular Cell Biology. 4th edition.

    New York: W. H. Freeman; 2000. Section 17.7, Protein Glycosylation in the ER and

    Golgi Complex. Retrieved from https://www.ncbi.nlm.nih.gov/books/NBK21744/

Low, S. C., Shaimi, R., Thandaithabany, Y., Lim, J. K., Ahmad, A. L., & Ismail, A. (2013). Electrophoretic interactions between nitrocellulose membranes and proteins: Biointerface analysis and protein adhesion properties. *Colloids and Surfaces B: Biointerfaces*, *110*, 248–253. Retrieved from https://doi.org/10.1016/j.colsurfb.2013.05.001

Mackenzie, J. M., Jones, M. K., & Westaway, E. G. (1999). Markers for trans-Golgi membranes and the intermediate compartment localize to induced membranes with distinct replication functions in flavivirus-infected cells. *Journal of Virology*, *73*(11), 9555–9567. Retrieved from http://www.ncbi.nlm.nih.gov/pubmed/10516064%0Ahttp://www.pubmedcentral.nih.gov/articlerender.fcgi?artid=PMC112990

Marciano-Cabral, F., & Cabral, G. A. (2007). The immune response to Naegleria fowleri amebae and pathogenesis of infection. *FEMS Immunology and Medical Microbiology*, *51*(2), 243–259. Retrieved from https://doi.org/10.1111/j.1574-695X.2007.00332.x

Martínez-Castillo, M., Cárdenas-Zúñiga, R., Coronado-Velázquez, D., Debnath, A., Serrano-Luna, J., & Shibayama, M. (2016). Naegleria fowleri after 50 years: Is it a neglected pathogen? *Journal of Medical Microbiology*, *65*(9), 885–896. Retrieved from https://doi.org/10.1099/jmm.0.000303

Model, M. A., Reese, J. L., & Fraizer, G. C. (2009). Measurement of wheat germ agglutinin binding with a fluorescence microscope. *Cytometry Part A*, *75*(10), 874–881. Retrieved from https://doi.org/10.1002/cyto.a.20787

Muthamilarasan, M., Mangu, V. R., Zandkarimi, H., Prasad, M., & Baisakh, N. (2016). Structure, organization and evolution of ADP-ribosylation factors in rice and foxtail millet, and their expression in rice. *Scientific Reports*, *6*(December 2015), 1–13. Retrieved from https://doi.org/10.1038/srep24008

Nickel, W., Brügger, B., & Wieland, F. T. (2002). Vesicular transport: the core machinery of

COPI recruitment and budding. *Journal of Cell Science*, *115*(Pt 16), 3235–3240.

Retrieved from http://www.ncbi.nlm.nih.gov/pubmed/12140255

Osada, N., Kohara, A., Yamaji, T., Hirayama, N., Kasai, F., Sekizuka, T., … Hanada, K.

(2014). The Genome Landscape of the African Green Monkey Kidney-Derived Vero

Cell Line. *DNA Research*, *21*(6), 673–683. Retrieved from

https://doi.org/10.1093/dnares/dsu029

Pelham, H. R. (1991). Multiple targets for brefeldin A. *Cell* , *67:449-451*, 449–451.

Popoff, V., Adolf, F., Brugger, B., & Wieland, F. (2011). COPI Budding within the Golgi

Stack. *Cold Spring Harbor Perspectives in Biology*, 1–20.

https://doi.org/10.1101/cshperspect.a005231

Rohde, J., Emschermann, F., Knittler, M. R., & Rziha, H. J. (2012). Orf virus interferes with

MHC class I surface expression by targeting vesicular transport and Golgi. *BMC

Veterinary Research*, *8*(1), 1. Retrieved from https://doi.org/10.1186/1746-6148-8-114

Schuster, F. L. (2002). Cultivation of Pathogenic and Opportunistic Free-Living Amebas.

CLINICAL MICROBIOLOGY REVIEWS, *15*(3), 342–354. Retrieved from

https://doi.org/10.1128/CMR.15.3.342

Sohn, H. J., Kim, J. H., Shin, M. H., Song, K. J., & Shin, H. J. (2010). The Nf-actin gene is

an important factor for food-cup formation and cytotoxicity of pathogenic Naegleria

fowleri. *Parasitology Research*, *106*(4), 917–924. Retrieved from

https://doi.org/10.1007/s00436-010-1760-y

Suda, Y., & Nakano, A. (2012). The Yeast Golgi Apparatus. *Traffic*, *13*(4), 505–510.

Retrieved from https://doi.org/10.1111/j.1600-0854.2011.01316.x

Visvesvara, G. S. (2010). Free-Living Amebae as Opportunistic Agents of Human Disease.

Journal of Neuroparasitology, *1*(May), 1–13. Retrieved from

https://doi.org/10.4303/jnp/n100802

Vivian, J. T., & Callis, P. R. (2001). Mechanisms of tryptophan fluorescence shifts in

    proteins. *Biophysical Journal*, *80*(5), 2093–2109. Retrieved from

    https://doi.org/10.1016/S0006-3495(01)76183-8

Wang, C., Ho, P. C., & Lim, L. Y. (2010). Wheat germ agglutinin-conjugated markers.

    International Journal of Pharmaceutics, *400*(1–2), 201–210. Retrieved from

    https://doi.org/10.1016/j.ijpharm.2010.08.023

Warren, G. (1993). Membrane Partitioning. *Annual Review of Biochemistry*, *62*, 323–348.

    Retrieved from https://doi.org/10.1146/annurev.bi.62.070193.001543

Xu, H., Su, W., Cai, M., Jiang, J., Zeng, X., & Wang, H. (2013). The Asymmetrical

    Structure of Golgi Apparatus Membranes Revealed by In situ Atomic Force

    Microscope. *PLoS ONE*, *8*(4), 1–10. Retrieved from

    https://doi.org/10.1371/journal.pone.0061596

Yuan, F., Xiong, G., Cohen, N. A., & Cohen, A. S. (2017). Optimized Protocol of Methanol

    Treatment for Immunofluorescent Staining in Fixed Brain Slices. *Applied*

    Immunohistochemistry and Molecular Morphology, *25*(3), 221–224. Retrieved from

    https://doi.org/10.1097/PAI.0000000000000293

Zeeh, J. C., Zeghouf, M., Grauffel, C., Guibert, B., Martin, E., Dejaegere, A., & Cherfils, J.

    (2006). Dual specificity of the interfacial inhibitor brefeldin A for arf proteins and Sec7

    domains. *Journal of Biological Chemistry*, *281*(17), 11805–11814. Retrieved from

    https://doi.org/10.1074/jbc.M600149200

Zyserman, I., Mondal, D., Sarabia, F., McKerrow, J. H., William, & R. Roush, and A. D.

    (2016). Identification of Cysteine Protease Inhibitors as New Drug Leads against

    Naegleria fowleri. *Experimental Parasitology*, *5*(6), 36–41. Retrieved from

    https://doi.org/10.1016/j.exppara.2018.03.010.Identification

Zysset-Burri, D. C., Müller, N., Beuret, C., Heller, M., Schürch, N., Gottstein, B., & Wittwer,

    M. (2014). Genome-wide identification of pathogenicity factors of the free-living

amoeba Naegleria fowleri. *BMC Genomics*, *15*(1), 1–15. Retrieved from

https://doi.org/10.1186/1471-2164-15-496

<u>Vita</u>

Tyler Matthias Poe was born November 11, 1991 in Ranson, West Virginia and is an America citizen. He went on to graduate from James Wood High School, Winchester, Virginia in 2010 with an Advanced High School Diploma where he also received a Woody Herman Jazz Award. He continued his education at James Madison University, Harrisonburg, Virginia graduating in 2015 where he received a Bachelor of Science degree in Biology.